Solid-State NMR Analysis of the PGLa Peptide Orientation in DMPC Bilayers: Structural Fidelity of ^{2}H-Labels versus High Sensitivity of ^{19}F-NMR

Erik Strandberg,* Parvesh Wadhwani,* Pierre Tremouilhac,* Ulrich H. N. Dürr,† and Anne S. Ulrich*†
*Institute for Biological Interfaces, Forschungszentrum Karlsruhe, 76344 Eggenstein-Leopoldshafen, Germany; and
†Institute of Organic Chemistry, University of Karlsruhe, 76131 Karlsruhe, Germany

ABSTRACT The structure and alignment of the amphipathic α-helical antimicrobial peptide PGLa in a lipid membrane is determined with high accuracy by solid-state ^{2}H-NMR. Orientational constraints are derived from a series of eight alanine-3,3,3-d_3-labeled peptides, in which either a native alanine is nonperturbingly labeled ($4\times$), or a glycine ($2\times$) or isoleucine ($2\times$) is selectively replaced. The concentration dependent realignment of the α-helix from the surface-bound "S-state" to a tilted "T-state" by 30° is precisely calculated using the quadrupole splittings of the four nonperturbing labels as constraints. The remaining, potentially perturbing alanine-3,3,3-d_3 labels show only minor deviations from the unperturbed peptide structure and help to single out the unique solution. Comparison with previous ^{19}F-NMR constraints from 4-CF_3-phenylglycine labels shows that the structure and orientation of the PGLa peptide is not much disturbed even by these bulky nonnatural side chains, which contain CF_3 groups that offer a 20-fold better NMR sensitivity than CD_3 groups.

INTRODUCTION

Solid-state NMR is a powerful tool to resolve the three-dimensional structures of membrane-active peptides embedded in lipid bilayers (1,2). For simple α-helical or β-stranded peptides, it is straightforward to collect a number of orientational constraints, from which the molecular conformation can be verified and its membrane alignment and dynamic behavior deduced (3). For each constraint, a selective isotope label has to be placed into a suitable position on the peptide, where it reflects its overall fold. Nonperturbing ^{15}N- and ^{13}C-isotopes are conveniently substituted in the backbone, and ^{2}H-labels can be utilized in the side chains. For the latter, alanine-3,3,3-d_3 (Ala-d_3) is most suitable, since the methyl group is attached directly to the backbone and reflects the orientation of the entire peptide segment (4,5).

A drawback of these conventional isotopes is their low sensitivity, which calls for large amounts of material, high peptide concentration in the sample, and comparatively long measurement times. Fluorine, on the other hand, is a nucleus with much higher NMR sensitivity, though this nonnatural label might disturb the system (3,6). Several peptide structures have been resolved by ^{19}F-NMR, whereby the most successful approach is based on 4-CF_3-phenylglycine (CF_3-Phg) side chains, which are conceptually analogous to Ala-d_3. (7–11). Here, we have carried out a comprehensive ^{2}H-NMR structure analysis of a membrane-bound antimicrobial peptide labeled with Ala-d_3 to compare these results with an analogous set of ^{19}F-NMR data based on an earlier CF_3-Phg study. The respective advantages and disadvantages of the two approaches will be discussed in terms of structural fidelity and experimental sensitivity.

Submitted September 7, 2005, and accepted for publication November 17, 2005.

Address reprint requests to Anne S. Ulrich, E-mail: anne.ulrich@ibg.fzk.de.

0006-3495/06/03/1676/11 $2.00

Membrane-active antimicrobial peptides with typically 10–50 amino acids are found in many organisms as part of the immune system to defend the host against invading bacteria and other microorganisms (12–15). These peptides kill bacteria presumably by disrupting their cell membranes. They tend to have an overall amphiphilic structure, which explains their high affinity for lipid bilayers. To understand their detailed mode of action, it is important to examine their structure in association with membranes at a molecular level, for which solid-state NMR is particularly well suited (1). The peptide PGLa (GMASKAGAIAGKIAKVALKAL-NH_2) is found in the skin of *Xenopus laevis* (16–18) and belongs to the magainin family (19). The amino acid sequence suggests an amphiphilic α-helical structure with charged lysine side chains on one side and hydrophobic residues on the opposite face (see Fig. 1). This conformation was confirmed by ^{1}H-NMR in detergent micelles, and by solid-state ^{15}N-NMR in the membrane-bound state (10,20). Using ^{15}N-labels in the peptide backbone, a flat surface alignment was demonstrated for the helix, although with a large margin of error and no information on its azimuthal rotation.

More recently, our ^{19}F-NMR analysis of CF_3-Phg substituted peptides yielded not only the tilt angle and azimuthal rotation of PGLa, but also revealed a concentration-dependent realignment in the membrane (9–11). It appears that increasing peptide concentration triggers a conversion from a monomeric surface-bound "S-state", with the helix axis aligned ~90° with regard to the bilayer normal, to a tilted "T-state" with a tilt angle of ~120°, whereby the amidated C-terminus of the α-helix becomes obliquely immersed into the bilayer. This novel T-state was rationalized in terms of oligomerization, given that PGLa and other related peptides are prone to homo- or heterodimerization (21–23). According to the commonly

doi: 10.1529/biophysj.105.073858

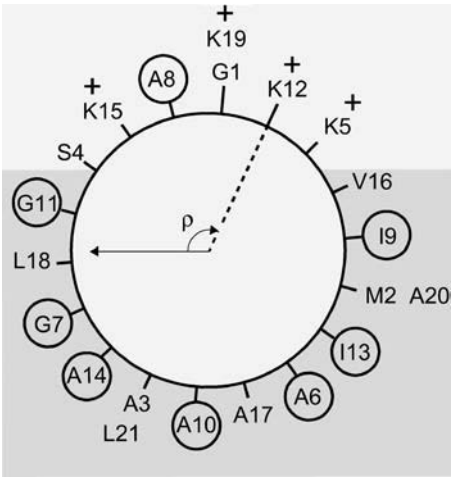

FIGURE 1 Helical wheel representation of the amphiphilic PGLa peptide, displayed here with the correct azimuthal rotation angle $\rho = 115°$ as it was found to reside in the membrane (*dark shaded box*). The positions labeled with Ala-d_3 are marked with circles, and the charged lysines with ''+''.

accepted picture of antimicrobial peptides, a reorientation may have been expected to lead to a fully upright transmembrane alignment in the so-called immersed ''I-state'' (with a corresponding angle of ~0°), as predicted by the Shai-Matzusaki-Huang model of antimicrobial function (24–26). Instead, the observation of an oblique tilt angle was interpreted as indirect evidence that PGLa might rather dimerize in the membrane under the conditions studied. In this study, we wanted to confirm the unexpected realignment seen by ^{19}F-NMR, and to determine the respective tilt angles with higher accuracy.

Here, a comprehensive ^{2}H-NMR structure analysis is carried out on PGLa, using a series of peptides labeled with Ala-d_3 in place of Ala, Gly, or Ile (Table 1). Substitution of a native Ala by Ala-d_3 will obviously cause no structural perturbation at all. This ^{2}H-NMR approach, called GALA (geometric analysis of labeled alanines), has previously been used on transmembrane peptides (4,5,27–29). A similar approach based on dipolar waves was also presented by Opella et al. (30). To our knowledge, this is the first time that quadrupolar waves are applied to a peripherally bound membrane peptide with a potentially nonideal α-helix. Much attention is therefore paid to the error analysis, not only in terms of the global peptide structure but also with regard to the local deviation of any individual labeled position. The resulting ^{2}H-NMR model structure is then compared to our previous results from ^{19}F-NMR (10,11) and ^{15}N-NMR (11). The accuracy and reliability of the NMR data using the different labeling strategies will thus be critically assessed.

MATERIALS AND METHODS

Materials

Dimyristoylphosphatidylcholine (DMPC) was purchased from Alexis Biochemicals (Lausen, Switzerland) or Avanti Polar Lipids (Alabaster, AL), and deuterium-depleted water was from Acros (Schwerte, Germany) and Sigma-Aldrich (Taufkirchen, Germany). Ala-d_3 was purchased from Cambridge Isotope Laboratories (Andover, MA) and Fmoc-protected (31). PGLa was labeled at eight different positions, one at a time, replacing alanine, glycine, or isoleucine with Ala-d_3 (Table 1). All peptides were synthesized on an Applied Biosystems (Foster City, CA) 433A instrument, using standard solid phase Fmoc-protocols (32). The crude material was purified by high-performance liquid chromatography on a C18 column using an acetonitrile/water gradient. The identity of the products was confirmed by MALDI-TOF mass spectrometry. After purification, all peptides were ~95% pure.

Sample preparation

Oriented samples

Appropriate amounts of peptides and lipids were codissolved in ~400 μl methanol/$CHCl_3$ 1:1 (v/v) and spread onto 25 thin glass plates of dimensions 18 mm × 7.5 mm × 0.08 mm (Marienfeld Laboratory Glassware, Lauda-Königshofen, Germany). The plates were dried in air for 1 h, followed by drying under vacuum overnight. They were stacked and placed into a hydration chamber with 96% relative humidity at 48°C for 24–48 h, before wrapping the stack in parafilm and plastic foil for the NMR measurements.

Nonoriented samples

Appropriate amounts of peptides and lipids were codissolved in ~200 μl methanol/$CHCl_3$ 1:1 (v/v). In samples with a peptide/lipid ratio of P/L = 1:200, typically 2 mg peptide plus 140 mg lipid were used, and in 1:50 samples ~4 mg peptide plus 70 mg lipid. The solution was dried under a stream of N_2, followed by vacuum drying for overnight. Deuterium-depleted water was added to the dry lipid-peptide mixture to reach 50% by total

TABLE 1 Amino acid sequences of the peptides used and quadrupole splittings (in kHz) measured in PGLa-Ala-d_3/DMPC samples

Peptide	Labeled position	Sequence	P/L = 1:200*	P/L= 1:200†	P/L = 1:50‡
PGLaWT	None	GMASKAGAIAGKIAKVALKAL-NH_2			
PGLa6	Ala-6	GMASK-Ala-d_3-GAIAGKIAKVALKAL-NH_2	7.8	15.6	18.2
PGLa7	Gly-7	GMASKA-Ala-d_3-AIAGKIAKVALKAL-NH_2	4.8	9.6	2.5
PGLa8	Ala-8	GMASKAG-Ala-d_3-IAGKIAKVALKAL-NH_2	8.6	17.2	42.0
PGLa9	Ile-9	GMASKAGA-Ala-d_3-AGKIAKVALKAL-NH_2	2.6	5.2	30.0
PGLa10	Ala-10	GMASKAGAI-Ala-d_3-GKIAKVALKAL-NH_2	7.5	15.0	30.3
PGLa11	Gly-11	GMASKAGAIA-Ala-d_3-KIAKVALKAL-NH_2	18.5	37.0	52.1
PGLa13	Ile-13	GMASKAGAIAGK-Ala-d_3-AKVALKAL-NH_2	13.2	26.4	20.1
PGLa14	Ala-14	GMASKAGAIAGKI-Ala-d_3-KVALKAL-NH_2	13.3	26.6	21.5

*90° edge of Pake powder pattern.
†0° edge of Pake powder pattern.
‡Oriented samples aligned with the bilayer normal along B_0.

weight. The sample was thoroughly mixed by vortexing and freeze-thawed several times. It was then transferred into a small polyethylene bag that was heat-sealed and placed into a second sealed plastic bag to avoid dehydration during NMR experiments. When not used for NMR experiments, the samples were stored at −20°C.

NMR spectroscopy

All measurements were carried out on a Bruker Avance 500 MHz NMR spectrometer (Bruker BioSpin, Rheinstetten, Germany) at 308 K. ^{31}P-NMR was performed at a frequency of 202.5 MHz using a Hahn echo sequence with phase cycling (33) with a 7 μs 90° pulse, 30 μs echo time, 2 s relaxation delay time, 100 kHz spectral width, 4096 data points, and proton decoupling using tppm20 (34). Typically, 128 scans were collected, and spectra were processed by left-shifting the free induction decay to start at the echo maximum, zero filling to 16,384 data points, and a 100 Hz exponential multiplication before Fourier transformation.

^{2}H-NMR experiments were performed at 76.77 MHz using a quadrupole echo sequence (35) with a 4.5 μs 90° pulse, an echo delay of 30 μs, an 80 ms relaxation delay time, 250 kHz spectral width, and 2048 data points. Between 300,000 and 1,000,000 scans were collected. Acquisition was started before the echo, and the time domain data was left-shifted to get the free induction decay starting at the echo maximum before further processing by zero filling to 16,384 data points and a 200 Hz exponential multiplication followed by Fourier transformation.

Structure calculations

The measured NMR parameters (quadrupole splittings of Ala-d_3, and ^{19}F-^{19}F dipole couplings of CF_3-Phg) were compared to a model of the peptide as an ideal α-helix. To determine the helix tilt angle τ, the azimuthal rotation ρ around the helix axis, and the order parameter S_{mol}, a least-squares fit was performed to find the globally smallest root mean-square deviation (rmsd) between the experimental and calculated NMR parameters (5,8,10,36). Further analysis of this rmsd minimum was performed using the GALA approach described earlier (4,5), which allows a graphical visualization of the error range for each labeled position.

To describe the peptide alignment in a membrane, the tilt angle τ defines the angle between the peptide helix axis and the bilayer normal. To be consistent with our earlier PGLa analysis (10,11), but in contrast to earlier definitions in Strandberg et al. (2004), the azimuthal angle ρ is defined as a right-handed rotation around the helix axis, with the axis directed from the N- to C-terminus. Here, $\rho = 0°$ is defined as the orientation when the vector projecting radially from the helix axis to the C^{α} atom of Lys-12 is aligned parallel to the membrane plane, as illustrated in Fig. 1. The angles describing the orientation of the C^{α}-C^{β} bond were for all residues taken as $\beta = 121.1°$ and $\alpha = 53.2°$, as deduced from an α-helical polyalanine model constructed in SYBYL using $\phi = -58°$ and $\psi = -47°$ (10). Here, β is the angle between the bond vector and the peptide axis, and α is the angle between the bond vector and the vector from the peptide axis to the C^{α} atom. The quadrupole coupling constant used was $e^2qQ/h = 167$ kHz (37). Since signs of the ^{2}H quadrupole splittings were not available, the absolute values were used in the analysis, whereas signs of the ^{19}F dipole couplings were accessible from the anisotropic chemical shift seen in the same one-pulse spectra (10).

The order parameter S_{mol} describes local internal oscillations and global wobbling motions of the molecule. Its effect in our calculations is to reduce all splittings by a constant factor, assuming a uniaxial ordering tensor.

RESULTS

Choice of oriented or nonoriented samples

Orientational constraints are most readily extracted from macroscopically oriented membrane samples. Provided that a well-oriented peptide undergoes long-axial rotation about the membrane normal, these parameters are also available from nonoriented multilamellar lipid dispersions (5,8,38). Samples for ^{2}H-NMR with PGLa embedded in DMPC were prepared both ways. The ^{31}P-NMR line shapes of all nonoriented samples showed a single lamellar phase with no indication of any isotropic or nonlamellar signals. For oriented samples, ^{31}P was used to determine the degree of orientation of the lipids. Typically, the well-oriented peak at low field contributed 70–80% to the integrated intensity, with the rest originating from nonoriented parts of the sample.

The ^{2}H-NMR spectra of oriented samples showed orientation-dependent quadrupole splittings. When the glass plates were oriented with their normal parallel to the magnetic field, the splittings were twice as large as for an orientation of the sample normal perpendicular to the field direction. This was the case at both peptide/lipid ratios (P/L) of 1:200 and 1:50, indicating that the peptides are rotating fast around the bilayer normal at 35°C in the liquid crystalline state of DMPC, as previously seen with ^{19}F-NMR (10,11). Nonoriented samples showed characteristic Pake patterns with splittings close to the ones in (perpendicularly) oriented samples. These results show that the peptides are well oriented and rotating fast, hence the same information can be obtained from liquid crystalline nonoriented samples as from oriented samples.

In previous ^{19}F-NMR studies of PGLa in lipid systems, we had used only oriented samples. However, as they are harder to prepare with the large amount of material required for the less sensitive ^{2}H-NMR measurements especially at low peptide concentration, we decided to use nonoriented dispersion samples at P/L = 1:200 and oriented samples at P/L = 1:50.

^{2}H-NMR results

The ^{2}H-NMR spectra of PGLa labeled at eight different positions with Ala-d_3 are shown in Fig. 2, for two different concentrations of peptides in DMPC. A P/L of 1:200 will be denoted as a ''low'' peptide concentration, whereas P/L = 1:50 is called ''high'' concentration. At low peptide concentration, the Pake pattern from the peptide is seen in all spectra, besides a sharp isotropic component due to traces of HDO in the hydrated samples. In some cases, the peptide splitting is too small to be resolved and contributes to the isotropic peak. There is also a low intensity component with a splitting of ~26 kHz, which is attributed to natural abundance deuterons in the lipids, as demonstrated by ^{2}H-NMR of pure lipid samples (data not shown). At high peptide concentration, a single dominant splitting is seen from the peptides in the oriented samples. The central component is smaller, as there is no excess water in these samples. In nonoriented samples, the main peak originates from parts of the membrane with the bilayer normal perpendicular to the magnetic field, whereas oriented samples are measured with their normal parallel to the magnetic field. Therefore, for comparison, the splittings for nonoriented samples should be

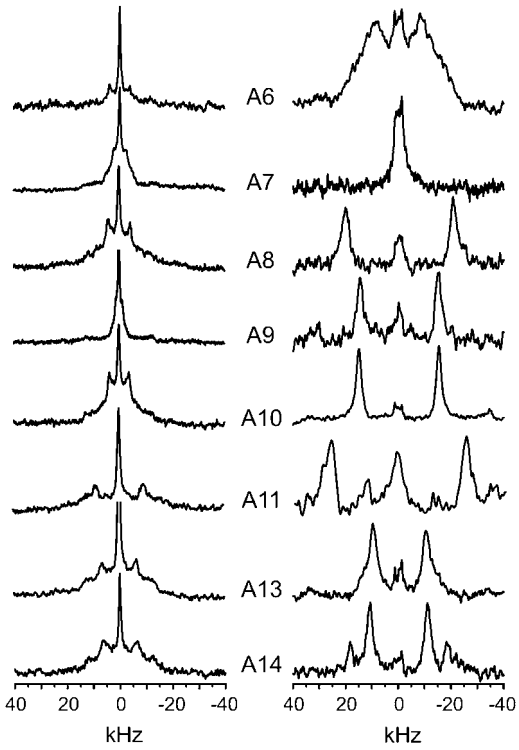

FIGURE 2 ^{2}H-NMR spectra of PGLa labeled with Ala-d_3 in eight different positions (as numbered) and reconstituted in DMPC at P/L = 1:200 (*left panel*), and 1:50 (*right panel*). The samples with low peptide concentrations were prepared as multilamellar lipid dispersions and show Pake patterns, whereas all samples with high concentration were prepared as macroscopically oriented membranes and show sharp splittings.

doubled. The peptide quadrupole splittings of all spectra are listed in Table 1. Since the splittings for any one label are different at low and high peptide concentration, this clearly indicates a concentration-dependent realignment of PGLa in the lipid bilayer.

It is generally possible to describe the alignment and dynamics of a peptide in the membrane by three parameters, namely the tilt angle τ of the helix axis with respect to the bilayer normal, the azimuthal rotation angle ρ around the helix axis, and the molecular order parameter S_{mol} (1,3–5, 7,8,10,11,36,39). Given that the effective (time-averaged) quadrupole tensor is collinear with the C-CD_3 axis in the molecular frame of PGLa, at least three orientational constraints are required to determine the three unknown parameters τ, ρ, and S_{mol}. In practice, more than three are needed, since the sign of a quadrupole splitting is not accessible, which leads to multiple solutions (40–43). It was found in a previous study that four labeled positions gave reliable results (5).To perform the structure analysis, the conformation of the peptide in the bilayer has to be known. PGLa was shown by circular dichroism to have a random structure in solution and to form an α-helix in the presence of lipid bilayers (10,44,45). ^{1}H-NMR confirmed an α-helix between residues 6 and 21 when PGLa was associated with DPC micelles (20). We therefore assumed an ideal (polyalanine) α-helix as a model structure for PGLa, to fit the quadrupole splittings of the different labeled positions in the peptide. In a grid search for the best-fit structure, the theoretical quadrupole splittings are calculated for different values of τ, ρ, and S_{mol}. The parameters τ and ρ are changed in steps of 0.1°, and S_{mol} in steps of 0.01 to find the lowest rmsd with regard to the experimental data.

Helix alignment at low peptide concentration

Native alanine positions

The substitution of ^{1}H by ^{2}H does not perturb the chemical properties of a molecule. Thus, a substitution of Ala by Ala-d_3 will not affect the molecular behavior of wild-type PGLa. However, when any other amino acid (in this case Gly or Ile) is replaced by Ala-d_3, such mutation might change the properties of the peptide. Therefore, the ^{2}H-NMR data analysis was first performed by taking into account only the orientational constraints from the four native Ala positions in the sequence, i.e., using the quadrupole splittings from Ala-6, Ala-8, Ala-10, and Ala-14. For a P/L = 1:200, this analysis produces a peptide structure with a helix tilt angle $\tau = 98°$, a rotation angle $\rho = 115°$, and an order parameter $S_{mol} = 0.66$ (Table 2). This result corresponds to an alignment of the peptide helix almost flat on the membrane surface in the so-called S-state (24,26), with the charged lysine side chains pointing up toward the water (Fig. 1). The numerical value of the tilt angle being higher than 90° means that the amidated C-terminus is inserted slightly deeper into the membrane than the charged N-terminus. This structure is in good agreement with our previous ^{19}F-NMR analysis, where a tilt angle $\tau \approx 89°$, a rotation $\rho \approx 115°$, and an order parameter $S_{mol} \approx 0.6$ had been obtained (10). Notably, the signs of the four quadrupole splittings used in our ^{2}H-NMR analysis are unknown and may produce additional solutions as artifacts, whereas the signs of the four dipolar splittings of CF_3-Phg had been directly accessible via the ^{19}F chemical shift anisotropy (10). Nevertheless, the current set of four ^{2}H-NMR constraints gives an rmsd of 1.3 kHz, which is convincingly small for this solution to be unique and reliable.

The quality of the fits can be assessed using two-dimensional error plots as well as quadrupolar waves. Fig. 3 *A* shows the error plot for the fit using the four native Ala-d_3 labels. Here, the rmsd error (in kHz) is illustrated by a grayscale for all combinations of τ and ρ. If we had also wanted to display the dependence on the order parameter, this would require a three-dimensional error plot, hence we only shown the τ/ρ map obtained for the best-fit order parameter value $S_{mol} = 0.66$. There exist several minima with an rmsd below 2.0 kHz since the signs of the four quadrupole splittings are not known, but the solution with a tilt angle near 100° is clearly the best fit. The corresponding quadrupolar wave is shown in Fig. 3 *B* and represents the

TABLE 2 Best-fit orientation parameters for PGLa in DMPC; potentially perturbing substitutions are highlighted

P/L	Labels used	Tilt angle τ (°)	Rotation angle ρ (°)	S_{mol}	rmsd (kHz)
1:200	CD_3 at Ala-6, Ala-8, Ala-10, Ala-14	98	115	0.66	1.3
	CD_3 at Ala-6, ***Gly-7***, Ala-8, Ala-10, ***Gly-11***, Ala-14	98	115	0.69	1.4
	CD_3 at Ala-6, Ala-8, ***Ile-9***, Ala-10, ***Ile-13***, Ala-14	98	114	0.68	2.2
	CD_3 at Ala-6, ***Gly-7***, Ala-8, ***Ile-9***, Ala-10, ***Gly-11***, ***Ile-13***, Ala-14	98	115	0.70	2.0
	CF_3 at ***Ile-9, Ala-10, Ile-13, Ala-14***	89	116	0.63	0.3
1:50	CD_3 at Ala-6, Ala-8, Ala-10, Ala-14	126	110	0.75	0.5
	CD_3 at Ala-6, ***Gly-7***, Ala-8, Ala-10, ***Gly-11***, Ala-14	127	109	0.74	1.0
	CD_3 at Ala-6, Ala-8, ***Ile-9***, Ala-10, ***Ile-13***, Ala-14	124	112	0.78	0.9
	CD_3 at Ala-6, ***Gly-7***, Ala-8, ***Ile-9***, Ala-10, ***Gly-11***, ***Ile-13***, Ala-14	126	111	0.78	1.2
	CF_3 at ***Ile-9, Ala-10, Ile-13, Ala-14***	123	95	0.63	0.2

unperturbed peptide structure ($\tau = 98°$, $\rho = 115°$, $S_{mol} = 0.66$). Here, the hypothetical quadrupole splittings are calculated for each position around the helical wheel and displayed on a curve from 0° to 360°. None of the experimental data points deviate significantly from the theoretical wave, which confirms that the labeled stretch is consistent over its full length with an unperturbed α-helical conformation.

The experimental error in the quadrupole splittings is estimated to be no more than 1 kHz, as found by repeated measurements on a sample or by use of duplicate samples. All rmsd values below this must be called ''good'' fits. It should also be noted that our analysis is based on the assumption of an ideal α-helical structure. Slight deviations are expected for amphiphilic peptides at the membrane surface; hence even larger rmsd values may be acceptable. In a previous study on uniformly hydrophobic transmembrane model peptides, the fit to an ideal helix had been justified by the very small rmsd values of typically <1 kHz found for such a model (4,5). For PGLa at 1:200, the error in τ and ρ is $\sim\pm3°$ in both cases, according to the area in the error plot that covers an rmsd of 1 kHz around the best fit.

Glycine or isoleucine substituted with alanine

When the two Gly → Ala-d_3 substitutions were included in the analysis at P/L = 1:200, the same best-fit values (within the error of the method) were found as when only nonperturbing native Ala labels were used (Table 2). Likewise, when two Ile → Ala-d_3 substitutions were included, the same best-fit values were obtained, although with a slightly higher rmsd error of 2.2 kHz. When all eight labeled positions were combined, the best-fit values of τ, ρ, and S_{mol} remained the same as in the entirely unperturbed structure, as seen in Table 2. The corresponding error plot in Fig. 3 *C* is now showing one clearly defined global minimum, and the many shallow minima of Fig. 3 *A* have disappeared. The additional data from the potentially perturbing labels thus confirm the unique and well-defined orientation of PGLa. In the quadrupolar wave plot in Fig. 3 *B*, the experimental splittings from the Gly or Ile positions (open symbols) lie close to the original curve calculated from the native Ala-d_3 labels alone (solid symbols). We conclude that the structure and orientation of PGLa at 1:200 are not influenced by the substitution of a small glycine residue nor a bulky isoleucine side chain by an alanine.

Helix alignment at high peptide concentration

Native alanine positions

At a high peptide concentration of P/L = 1:50, the orientation parameters derived as the best-fit solution are given in Table 2. Again, we initially used only the four labels in native Ala positions to obtain a reliable structure, and the result is clearly different from that at low peptide concentration. The best-fit values are $\tau = 126°$, $\rho = 110°$, and $S_{mol} = 0.75$. This means that the tilt angle is ~30° larger than at the low peptide concentration, whereas the azimuthal rotation angle and the order parameter do not change much. In the corresponding error plot of Fig. 4 *A*, this minimum is the deepest, with an rmsd of only 0.5 kHz. This error is even smaller than the intrinsic experimental error. There are also two other minima corresponding to tilt angles τ of ~25° and 60°, but with considerably larger errors. We are confident that $\tau = 126°$ is the correct solution for P/L = 1:50, since a similar picture was obtained by ^{19}F-NMR from four Phg-CF_3 labels for which the signs of the dipolar splittings were known (11).

Glycine or isoleucine substituted with alanine

We next included the ^{2}H-NMR data from the Ile and Gly substitutions in the analysis at high peptide concentration, for comparison with the unperturbed structure. In the quadrupolar wave plot of Fig. 4 *B*, the curve represents the best fit derived from the splittings of the four native Ala positions only (solid symbols), whereas the other splittings of the potentially perturbing labels are displayed with open symbols. The data points from the substituted positions (Gly-7, Gly-11, Ile-9, and Ile-13) fit almost perfectly to the wave, and an independent best-fit analysis using all eight positions gave practically the same values ($\tau = 126°$, $\rho = 111°$, and $S_{mol} = 0.78$). The corresponding error plot in Fig. 4 *C* now shows a single well-defined minimum with an rmsd of 1.2 kHz. We thus conclude that also at high peptide concentration,

the substitution of Gly or Ile by Ala does not cause any significant perturbation.

DISCUSSION

In this study, we have used solid-state ^{2}H-NMR on selectively Ala-d_3 labeled PGLa to determine the orientation of this antimicrobial peptide in a lipid bilayer at different concentrations. First, we will assess the results in the light of those obtained previously on transmembrane peptides. Then we will compare the different PGLa structures at low and high peptide concentration. We will also include previous data from analogous ^{19}F- and ^{15}N-NMR studies on PGLa and examine the local deviations of these combined results. Finally, the different labeling strategies for solid-state NMR studies of membrane peptides will be critically discussed with regard to accuracy on the one hand, and practical aspects such as NMR sensitivity on the other hand.

Comparison of surface-bound and transmembrane peptides

In previous ^{2}H-NMR studies of the transmembrane model peptides WALP19 (GWW(LA)$_6$LWWA) and WALP23 (GWW(LA)$_8$LWWA) labeled with Ala-d_3, the helices were found to span the membrane with a small tilt angle τ of up to 8° (4,5). This tilt was found to depend on the hydrophobic thickness of the membrane, as it assumed a slightly larger value when the peptide was too long to span the lipid bilayer. The quality of fit of the NMR data was very good and deteriorated only when the peptide-lipid hydrophobic mismatch became significant. For WALP23 in DOPC, the rmsd error from eight labeled positions was below 0.5 kHz, meaning that the peptide forms a virtually ideal α-helix. For WALP23 in DMPC, and for WALP19 in DLPC, DMPC and DOPC, the rmsd was below 1.0 kHz. Only for a considerable mismatch was there a larger error. In a more recent study, similar transmembrane peptides KALP23, WLP23, and KLP23 were examined the same way in the same lipid bilayers, and their mismatch-dependent tilt between 4° and 12° also showed rmsd values below 1.0 kHz (46). These reports demonstrate that transmembrane α-helices are close to ideal, as expected, since breaking or even distorting a hydrogen bond in the hydrophobic environment would be expensive in terms of free energy.

In the case of PGLa, the amphiphilic α-helix is embedded in the membrane surface. It may be expected to be less symmetric in such location, since one side of the peptide faces a polar environment where the CO and NH groups could form hydrogen bonds with solvent molecules or with the lipid headgroups. It has been reported that in amphiphilic helices, the hydrogen bonds are shorter on the hydrophobic face than on the hydrophilic face (47,48), which would cause the helix to bend and deviate from the ideal model. In our study, such conformational effects were not taken into account, and the two helical turns from Ala-6 to Ala-14 were fitted to an ideal α-helical model of polyalanine, with torsion angles $\phi = -58°$ and $\psi = -47°$. Given the heterogeneous primary sequence of PGLa, the Ala residues in different

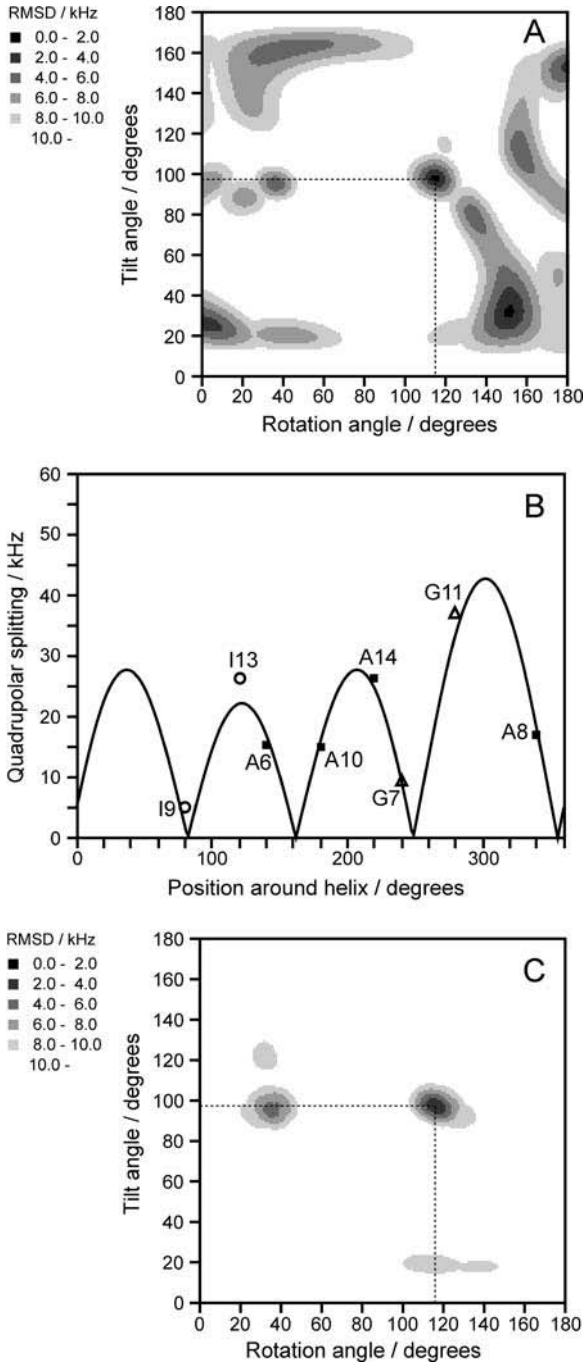

FIGURE 3 (*A*) Error plot for PGLa/DMPC at 1:200, using only the ^{2}H-NMR data from the four nonperturbing positions Ala-6, Ala-8, Ala-10, and Ala-14. (*B*) Quadrupolar wave plot, with the curve fitted only to the four native Ala positions (■). The experimental splittings from two Ile positions (○) and two Gly positions (△) are also shown, with residue numbers given next to the data points. (*C*) Error plot calculated from all eight labeled Ala-d_3 positions, showing a unique minimum that confirms the best-fit solution from panel *A*.

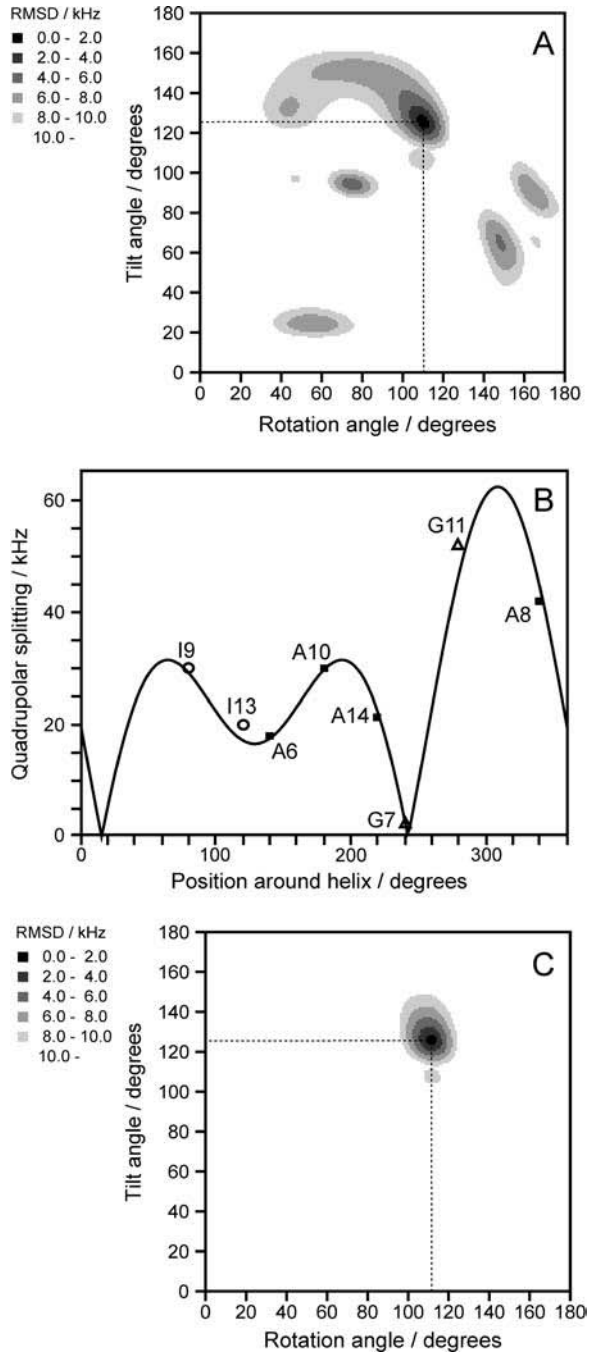

FIGURE 4 (*A*) Error plot for PGLa/DMPC at 1:50, using only the ^{2}H-NMR data from the four nonperturbing positions Ala-6, Ala-8, Ala-10, and Ala-14. (*B*) Quadrupolar wave plot, with the curve fitted only to the four native Ala positions (■). The experimental splittings from two Ile positions (○) and two Gly positions (△) are also shown, with residue numbers given next to the data points. (*C*) Error plot calculated from all eight labeled Ala-d_3 positions, showing a unique minimum that confirms the best-fit solution from panel *A*.

positions have different neighboring amino acids, which may further change their local torsion angles to some extent. In contrast, the WALP peptides are very regular, as all Ala have Leu neighbors. It is therefore not surprising that the rmsd values obtained here, on the order of a few kHz, are significantly larger than for the transmembrane helices. Indeed, in previous ^{19}F-NMR studies of PGLa and other peptides, we have carried out a systematic structure analysis based on different α-helical starting models, and it turned out that the uncertainty of the chosen conformational model introduced a larger error than the intrinsic experimental data (10,39).

Concentration-dependent realignment of PGLa

At a low concentration of P/L = 1:200, the best-fit structure based on the four native Ala residues only, shows that PGLa lies almost flat on the bilayer surface in the so-called S-state ($\tau = 98°$). The charged lysine residues point toward the aqueous layer and the hydrophobic residues are in contact with the lipid bilayer interior, as illustrated by the azimuthal rotation of the helical wheel in Fig. 1. At a high concentration of P/L = 1:50, the helix tilt angle τ increases by ~30 to 125°, whereas the azimuthal rotation angle ρ of 115° remains almost unchanged, and the order parameter S_{mol} increases slightly. This tilted state was first qualitatively observed by ^{19}F-NMR and called the T-state, and it has now been unambiguously confirmed by ^{2}H-NMR using unperturbed PGLa.

Besides labeling the four native Ala positions, Ala-d_3 was also used to substitute Gly-7, Gly-11, Ile-9, or Ile-13 (Table 1). When the orientational constraints from these labels are included in the structure analysis, their individual quadrupole splittings fit well to the quadrupolar wave from the four native Ala labels, both at low and high peptide concentration (Figs. 3 *B* and 4 *B*). This finding suggests that a substitution of Gly → Ala-d_3 or Ile → Ala-d_3 does not significantly affect the peptide conformation or its alignment in the membrane. In the case of monomeric PGLa at low concentration, the helix orientation appears to be dictated by the overall amphiphilicity of the peptide; hence a conservative mutation can be readily accommodated. At high peptide concentration, the picture may be regarded as more complex, given that the formation of antiparallel dimers has been invoked to explain the change in the peptide tilt angle (11). When a dimer is formed, we can now tell that the alignment and the crossing angle of the packed molecules are not affected by any of the substitutions made here. This may mean that either the dimer interface is rather soft and can accommodate such variations in the size of the side chain, or, alternatively, our mutations may simply not have involved the putative dimer interface. Note that Gly-7 and Gly-11 are located on the left side of the helical wheel in Fig. 1, whereas Ile-9 and Ile-13 are situated on the opposite side. None of the positions in the Ala-rich quadrant facing down (Ala-14 to Ala-6) have been targeted yet by any ^{2}H-NMR mutations. It is interesting to note that a related peptide K3, which had been designed on the basis of the PGLa sequence, was recently shown to form homodimers in the membrane-bound state via its Ala-rich surface (23,49).

Comparison with previous ^{15}N- and ^{19}F-NMR results

In a previous study, PGLa was labeled with ^{15}N in the amide bond of Gly-11, whose chemical shift was measured in oriented samples of PGLa/DMPC at P/L = 1:200 and 1:50 (10). ^{15}N is a nondisturbing isotope label, giving conformationally unperturbed results. A single ^{15}N label is sufficient to estimate the peptide tilt angle, but gives no information about the azimuthal rotation. In PGLa, the chemical shift changed from 40 ppm (referenced to $^{15}NH_4NO_3$) at low peptide concentration to 68 ppm at high concentration. This significant change suggested a realignment of the peptide helix from a tilt angle of $\tau \approx 90°$ to $\sim$115° (11), which is nicely compatible with the results from ^{2}H-NMR presented here. The analysis from a single ^{15}N-label is associated with a broad error in τ ($\pm$20°), since the relevant chemical shift anisotropy (CSA) interactions are not colinear with the helix axis, and since the principal axes values may differ slightly from one amino acid to another. A single ^{15}N label does not reveal the azimuthal rotation angle ρ either. A more comprehensive picture is available from the dipolar couplings of multiple NH bonds, which can be analyzed in terms of PISA (polarity index slant angle) wheels or dipolar waves (2,30) analogously to the quadrupolar waves presented here.

As a highly sensitive alternative to conventional isotopes, we have previously introduced ^{19}F-labeling for solid-state NMR structure analysis of membrane-active peptides (3,7–9,36,39,50). The structure and alignment of PGLa in DMPC bilayers was studied using four peptide analogs labeled with CF_3-Phg. The anisotropy of the homonuclear dipolar coupling (including its sign) within the CF_3 group is readily analyzed in a simple one-pulse experiment (10,11). The CF_3-Phg side chain consists of an aromatic ring that is directly connected to the C^α atom, with the CF_3 group at the *para* position. The CF_3 group is rigidly attached to the peptide backbone along the direction of the C^α-C^β bond. Orientational constraints from the CF_3 group thus reflect the behavior of the peptide backbone in an analogous manner as the CD_3 groups analyzed above. In the previous ^{19}F-NMR study of PGLa, we had selectively labeled positions Ile-9, Ala-10, Ile-13, and Ala-14, which have now been labeled with Ala-d_3 for ^{2}H-NMR.

From geometrical considerations, the CF_3 group in CF_3-Phg should be oriented with respect to the peptide backbone in the same way as the CD_3 group in Ala-d_3. Both the dipolar and quadrupolar spin interactions experience an angular dependence of $\frac{1}{2}(3\cos^2\theta - 1)$, where θ is the angle between the C^α-C^β bond vector and the magnetic field direction. When considering either label in the same position of the peptide sequence, the quadrupole splitting from the CD_3 group and the dipolar coupling from the CF_3 group should be related to one another by a constant factor of 5.3. This factor is the ratio between the maximum dipolar coupling $\Delta^0_{CF_3} = 15.8$ kHz of a rotationally averaged CF_3 group (10) and the maximum quadrupole splitting $\Delta^0_{CD_3} = 82$ kHz of a rotating CD_3 group (4,40,41). Provided that the peptide remains undistorted and has the same orientation in the bilayer in both labeled analogs, then the two types of splitting from any one position should be scaled by the same constant factor, with $\sim$5.3 times larger splittings in ^{2}H. We can thus compare the ^{19}F dipolar couplings reported previously (10,11) with the present ^{2}H quadrupole splittings in Table 3. In the current case, where the order parameters of the two data sets are slightly different, this factor will scale accordingly. For P/L = 1:200, the order parameter found for ^{19}F is 0.63, and for ^{2}H it is 0.67, thus giving a factor of 5.6. For P/L = 1:50, the order parameters are 0.63 and 0.78, respectively, giving a factor of 6.6.

At low peptide concentration, the ratios between the dipolar and quadrupole splittings at positions Ile-13 and Ala-14 are indeed close to the theoretical value. The small ^{19}F dipolar couplings at positions Ile-9 and Ala-10 were not well resolved and had thus been set to 0 kHz. From the ^{2}H-NMR data, we can now conclude that dipolar couplings of 1.0 and 2.8 kHz, respectively, would have been expected for these two CF_3-Phg substituents. It is indeed plausible that the CF_3 splitting at position Ile-9 is $\sim$1 kHz, which is indeed too small to be resolved in the dipolar triplet (data not shown, see Glaser et al. (10)). Only the CF_3-Phg label at position Ala-10 is not entirely consistent with the expected value. Nevertheless, when the signs of the quadrupole splittings are back-calculated from the best-fit values of the peptide tilt and rotation angles, the predicted signs for position Ile-13 and Ala-14 are the same as those that were directly observed by ^{19}F-NMR. These good correlations indicate that it is possible to use the sign of the NMR interaction (i.e., the CSA) observed in ^{19}F-NMR to refine the quadrupolar ^{2}H-NMR analysis for which the sign is inaccessible otherwise. Given the good correlation between the ^{2}H- and ^{19}F-NMR data at low peptide concentration (P/L = 1:200), it is not surprising that the calculated structures of PGLa are similar when based on either the ^{2}H or ^{19}F data in the analysis. Using four ^{19}F labels, the best fit in our earlier work had given $\tau \approx 89°$, $\rho \approx$

TABLE 3 Comparison of CD_3 quadrupole splittings and CF_3 dipolar couplings in PGLa (see text)

P/L	Labeled position	CD_3 (kHz)*	CF_3 (kHz)	CD_3/CF_3*
1:200	Ile-9	5.2†	0‡	n.a.
	Ala-10	15.0†	0‡	n.a.
	Ile-13	26.4†	+5.6	4.8
	Ala-14	26.6†	−5.4	4.9
1:50	Ile-9	30.0	−4.7	6.4
	Ala-10	30.3	−3.1	9.7
	Ile-13	20.1	−3.3	6.1
	Ala-14	21.5	−5.3	3.9

*Absolute values, no sign available.
†Nonoriented samples, Pake splittings multiplied by 2.
‡Too small to be experimentally resolved.

106°, and $S \approx 0.6$ (10), for which the corresponding dipolar wave is included here as a dotted line in Fig. 5 *A*.

At a high peptide concentration of P/L = 1:50, the picture is somewhat different. Table 3 shows that the ratio of the dipolar and quadrupole splittings deviates significantly from the expected factor (6.6 when taking the order parameter into account) at the two positions of Ala-10 and Ala-14. This is also seen in the wave plots of Fig. 5 *B*, where the ^{19}F data points of Ile-9 and Ile-13 are fully compatible with the unperturbed PGLa structure (*solid line*), whereas the CF_3-Phg substitutions at Ala-10 and Ala-14 deviate notably. We may suggest two possible explanations for this observation. It would appear reasonable that a bulky Ile side chain can be safely substituted by a similarly large CF_3-Phg, whereas a small Ala site cannot readily accommodate such bulky substituent (although this argument cannot be generalized to include all data at low peptide concentration). Alternatively, it may not be the type of amino acid that is susceptible to mutations but rather the mutated position on the helical wheel, which may be involved in the putative dimer interface at high peptide concentration. The helical wheel of Fig. 1 shows that Ala-10 and Ala-14 are adjacent to one another in the three-dimensional structure. Indeed, Ala-10 and Ala-14 have been demonstrated by REDOR distance measurements to form the dimer interface of the analogous peptide K3, whose sequence $(KIAGKIA)_3$ is derived from PGLa (23). Even though it is purely speculative to draw such analogy, the current ^{2}H- and ^{19}F-NMR data are consistent with the possibility that also PGLa may dimerize via its Ala-rich surface.

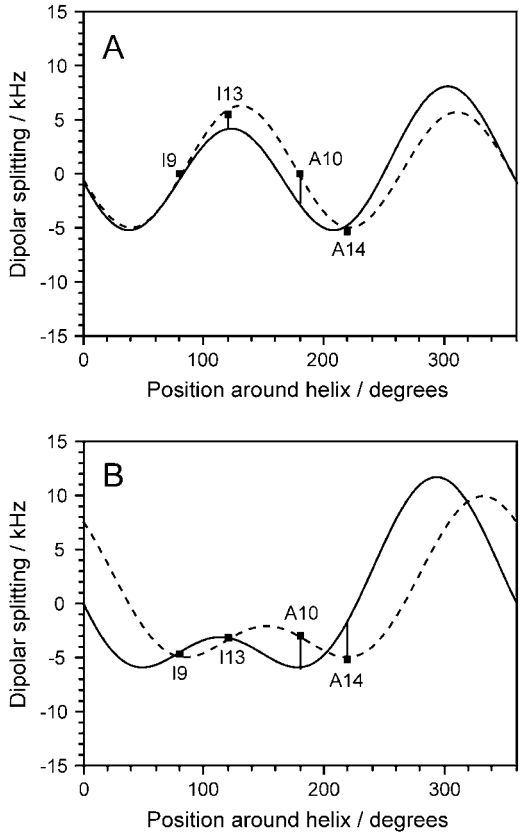

FIGURE 5 Dipolar wave plots of our current ^{2}H-NMR data at P/L = 1:200 (*A*) and P/L=1:50 (*B*), for comparison with our previous ^{19}F-NMR data on PGLa acquired with CF_3-Phg labels. The solid curves represent the unperturbed peptide structure as calculated from the best-fit ^{2}H-NMR parameters of native Ala substitutions, whereas the dotted curves are calculated from the best fit to the CF_3 data (solid squares, cf. Table 3). Deviations of any CF_3-Phg substituents from the ideal peptide structure are indicated.

It is obviously not advisable to use any amino acid substitutions for an NMR analysis when a structure needs to be i), exactly known, or when ii), the peptide is expected to oligomerize. Nevertheless, the comparison of our ^{2}H- and ^{19}F-NMR data shows that a rough picture of the peptide conformation and alignment is still accessible and the overall features are reliable, even when using nonnatural CF_3-Phg labels. That is, the values of τ, ρ, and S_{mol} calculated from the four CF_3-Phg substitutions are close to the results obtained by the four nonperturbing ^{2}H-NMR labels (Table 2). Hence the conclusions of our previous ^{19}F-NMR studies are still fully valid, namely that PGLa undergoes a concentration-dependent realignment in the membrane by ~30°, taking it from the surface-bound S-state to a novel tilted T-state. It has to be noted that the peptide analogs with a CF_3-Phg label at position 9, 10, 13, or 14 still exhibit an antimicrobial activity comparable to that of the wild-type PGLa (8). Only one label at position Ala-8 on the hydrophilic face exhibited a reduced activity and had thus been excluded from the earlier structure analysis (10).

^{19}F-NMR labeling strategy for peptides

The main advantage of using ^{19}F-labeled peptides is the exquisitely high sensitivity of ^{19}F-NMR and the lack of a natural abundance background. The results of our ^{2}H-NMR study demonstrate that for monomeric PGLa, the previously used ^{19}F-labels do not disturb the peptide-lipid system. CF_3-Phg is therefore a very useful label, which also provides the sign of the dipolar coupling via the CSA interaction, which is not available for the quadrupole splitting. Given the high sensitivity of ^{19}F-NMR, small amounts of peptide and short NMR acquisition times produce strong signals. It is therefore advantageous to use ^{19}F-labeled peptides for systematically monitoring a wide range of sample conditions, e.g., lipid composition, temperature, pH, and peptide concentration. For PGLa in DMPC, molar peptide/lipid ratios as low as 1:3000 have been examined that way. With increasing peptide concentration up to 1:8, a sigmoidal curve of NMR parameters was obtained suggesting a realignment at ~1:100 (9,11). When such ^{19}F-NMR studies indicate that under certain conditions some interesting structural changes occur, then some nonperturbing, but less sensitive labels like ^{15}N and ^{2}H, can be introduced to obtain a more accurate picture of the peptide under those selected conditions. Having acquired the two sets of ^{19}F- and ^{2}H-NMR data with the same

peptide, a direct comparison of their relative sensitivities shows that 0.25 mg of CF_3-Phg labeled PGLa gave a good signal in 2 h, whereas 2 mg of CD_3-labeled peptide gave an acceptable signal after 5 h. In practical terms, the theoretically expected 100-fold gain in sensitivity of ^{19}F-NMR over ^{2}H-NMR is thus reduced to an effective factor of 20, due to the favorable quadrupolar relaxation of deuterium allowing fast recycle delays (51).

We are grateful to Ralf Glaser and Carsten Sachse for useful discussions about PGLa peptides.

We thank the Deutsche Forschungsgemeinschaft and Centre for Functional Nanostructures for financial support.

REFERENCES

1. Strandberg, E., and A. S. Ulrich. 2004. NMR methods for studying membrane-active antimicrobial peptides. *Concept. Magnetic. Res. A.* 23A:89–120.
2. Opella, S. J., and F. M. Marassi. 2004. Structure determination of membrane proteins by NMR spectroscopy. *Chem. Rev.* 104:3587–3606.
3. Ulrich, A. S., P. Wadhwani, U. H. N. Dürr, S. Afonin, R. W. Glaser, E. Strandberg, P. Tremouilhac, C. Sachse, M. Berditchevskaia, and S. L. Grage. 2006. Solid state ^{19}F-nuclear magnetic resonance analysis of membrane-active peptides. *In* NMR spectroscopy of biological solids. A. Ramamoorthy, editor. CRC Press, Boca Raton, FL. 215–236.
4. Van der Wel, P. C. A., E. Strandberg, J. A. Killian, and R. E. Koeppe 2nd. 2002. Geometry and intrinsic tilt of a tryptophan-anchored transmembrane α-helix determined by ^{2}H NMR. *Biophys. J.* 83:1479–1488.
5. Strandberg, E., S. Özdirekcan, D. T. S. Rijkers, P. C. A. van der Wel, R. E. Koeppe 2nd, R. M. J. Liskamp, and J. A. Killian. 2004. Tilt angles of transmembrane model peptides in oriented and nonoriented lipid bilayers as determined by ^{2}H solid state NMR. *Biophys. J.* 86: 3709–3721.
6. Ulrich, A. S. 2000. High resolution ^{1}H and ^{19}F solid state NMR. *In* Encyclopedia of Spectroscopy and Spectrometry. J. Lindon, G. Tranter, and J. Holmes, editors. Academic Press, London. 813–825.
7. Salgado, J., S. L. Grage, L. H. Kondejewski, R. S. Hodges, R. N. McElhaney, and A. S. Ulrich. 2001. Membrane-bound structure and alignment of the antimicrobial β-sheet peptide gramicidin S derived from angular and distance constraints by solid state ^{19}F-NMR. *J. Biomol. NMR.* 21:191–208.
8. Afonin, S., R. W. Glaser, M. Berditchevskaja, P. Wadhwani, K. H. Gührs, U. Möllmann, and A. S. Ulrich. 2003. 4-Fluoro-phenylglycine as a label for ^{19}F-NMR structure analysis of membrane associated peptides. *ChemBioChem.* 4:1151–1163.
9. Glaser, R. W., and A. S. Ulrich. 2003. Susceptibility corrections in solid-state NMR experiments with oriented membrane samples. Part I: applications. *J. Magn. Reson.* 164:104–114.
10. Glaser, R. W., C. Sachse, U. H. Durr, P. Wadhwani, and A. S. Ulrich. 2004. Orientation of the antimicrobial peptide PGLa in lipid membranes determined from ^{19}F-NMR dipolar couplings of 4-CF_3-phenylglycine labels. *J. Magn. Reson.* 168:153–163.
11. Glaser, R. W., C. Sachse, U. H. Dürr, S. Afonin, P. Wadhwani, E. Strandberg, and A. S. Ulrich. 2005. Concentration-dependent realignment of the antimicrobial peptide PGLa in lipid membranes observed by solid-state ^{19}F-NMR. *Biophys. J.* 88:3392–3397.
12. Saberwal, G., and R. Nagaraj. 1994. Cell-lytic and antibacterial peptides that act by perturbing the barrier function of membranes. Facets of their conformational features, structure-function correlations and membrane-perturbing abilities. *Biochim. Biophys. Acta.* 1197:109–131.
13. Epand, R. M., and H. J. Vogel. 1999. Diversity of antimicrobial peptides and their mechanisms of action. *Biochim. Biophys. Acta.* 1462:11–28.
14. Hancock, R. E., and D. S. Chapple. 1999. Peptide antibiotics. *Antimicrob. Agents Chemother.* 43:1317–1323.
15. Van 't Hof, W., E. C. Veerman, E. J. Helmerhorst, and A. V. Amerongen. 2001. Antimicrobial peptides: properties and applicability. *Biol. Chem.* 382:597–619.
16. Hoffmann, W., K. Richter, and G. Kreil. 1983. A novel peptide designated PYLa and its precursor as predicted from cloned mRNA of *Xenopus laevis* skin. *EMBO J.* 2:711–714.
17. Soravia, E., G. Martini, and M. Zasloff. 1988. Antimicrobial properties of peptides from *Xenopus* granular gland secretions. *FEBS Lett.* 228:337–340.
18. Richter, K., H. Aschauer, and G. Kreil. 1985. Biosynthesis of peptides in the skin of *Xenopus laevis*: isolation of novel peptides predicted from the sequence of cloned cDNAs. *Peptides.* 6(Suppl. 3):17–21.
19. Zasloff, M. 1987. Magainins, a class of antimicrobial peptides from Xenopus skin: isolation, characterization of two active forms, and partial cDNA sequence of a precursor. *Proc. Natl. Acad. Sci. USA.* 84:5449–5453.
20. Bechinger, B., M. Zasloff, and S. J. Opella. 1998. Structure and dynamics of the antibiotic peptide PGLa in membranes by solution and solid-state nuclear magnetic resonance spectroscopy. *Biophys. J.* 74:981–987.
21. Hara, T., Y. Mitani, K. Tanaka, N. Uematsu, A. Takakura, T. Tachi, H. Kodama, M. Kondo, H. Mori, A. Otaka, F. Nobutaka, and K. Matsuzaki. 2001. Heterodimer formation between the antimicrobial peptides magainin 2 and PGLa in lipid bilayers: a cross-linking study. *Biochemistry.* 40:12395–12399.
22. Wakamatsu, K., A. Takeda, T. Tachi, and K. Matsuzaki. 2002. Dimer structure of magainin 2 bound to phospholipid vesicles. *Biopolymers.* 64:314–327.
23. Toke, O., R. D. O'Connor, T. K. Weldeghiorghis, W. L. Maloy, R. W. Glaser, A. S. Ulrich, and J. Schaefer. 2004. Structure of $(KIAGKIA)_3$ aggregates in phospholipid bilayers by solid-state NMR. *Biophys. J.* 87:675–687.
24. Matsuzaki, K. 1998. Magainins as paradigm for the mode of action of pore forming polypeptides. *Biochim. Biophys. Acta.* 1376:391–400.
25. Shai, Y. 1999. Mechanism of the binding, insertion and destabilization of phospholipid bilayer membranes by alpha-helical antimicrobial and cell non-selective membrane-lytic peptides. *Biochim. Biophys. Acta.* 1462:55–70.
26. Huang, H. W. 2000. Action of antimicrobial peptides: two-state model. *Biochemistry.* 39:8347–8352.
27. Jones, D. H., K. R. Barber, and C. W. M. Grant. 1998. The EGF receptor transmembrane domain: ^{2}H NMR study of peptide phosphorylation effects in a bilayer environment. *Biochemistry.* 37:7504–7508.
28. Whiles, J. A., R. Brasseur, K. J. Glover, G. Melacini, E. A. Komives, and R. R. Vold. 2001. Orientation and effects of mastoparan X on phospholipid bicelles. *Biophys. J.* 80:280–293.
29. Whiles, J. A., K. J. Glover, R. R. Vold, and E. A. Komives. 2002. Methods for studying transmembrane peptides in bicelles: consequences of hydrophobic mismatch and peptide sequence. *J. Magn. Reson.* 158:149–156.
30. Nevzorov, A. A., M. F. Mesleh, and S. J. Opella. 2004. Structure determination of aligned samples of membrane proteins by NMR spectroscopy. *Magn. Reson. Chem.* 42:162–171.
31. Carpino, L. A., and G. Y. Han. 1972. 9-Fluorenylmethoxycarbonyl amino protecting group. *J. Org. Chem.* 37:3404–3409.
32. Fields, G. B., and R. L. Noble. 1990. Solid-phase peptide synthesis utilizing 9-fluorenylmethoxycarbonyl amino acids. *Int. J. Pept. Protein Res.* 35:161–214.
33. Rance, M., and R. A. Byrd. 1983. Obtaining high-fidelity spin-1/2 powder spectra in anisotropic media—phase-cycled Hahn echo spectroscopy. *J. Magn. Reson.* 52:221–240.

34. Bennett, A. E., C. M. Rienstra, M. Auger, K. V. Lakshmi, and R. G. Griffin. 1995. Heteronuclear decoupling in rotating solids. *J. Chem. Phys.* 103:6951–6958.

35. Davis, J. H., K. R. Jeffrey, M. Bloom, M. I. Valic, and T. P. Higgs. 1976. Quadrupolar echo deuteron magnetic resonance spectroscopy in ordered hydrocarbon chains. *Chem. Phys. Lett.* 42:390–394.

36. Ulrich, A. S. 2005. Solid state ^{19}F-NMR methods for studying biomembranes. *Prog. Nucl. Magn. Reson. Spectrosc.* 46:1–21.

37. Davis, J. H. 1983. The description of membrane lipid conformation, order and dynamics by ^{2}H-NMR. *Biochim. Biophys. Acta.* 737:117–171.

38. Yamaguchi, S., T. Hong, A. Waring, R. I. Lehrer, and M. Hong. 2002. Solid-state NMR investigations of peptide-lipid interaction and orientation of a β-sheet antimicrobial peptide, protegrin. *Biochemistry.* 41:9852–9862.

39. Afonin, S., U. H. Dürr, R. W. Glaser, and A. S. Ulrich. 2004. 'Boomerang'-like insertion of a fusogenic peptide in a lipid membrane revealed by solid-state ^{19}F NMR. *Magn. Reson. Chem.* 42:195–203.

40. Ulrich, A. S., M. P. Heyn, and A. Watts. 1992. Structure determination of the cyclohexene ring of retinal in bacteriorhodopsin by solid-state deuterium NMR. *Biochemistry.* 31:10390–10399.

41. Ulrich, A. S., and A. Watts. 1993. ^{2}H-NMR lineshapes of immobilized uniaxially oriented membrane proteins. *Solid State Nucl. Magn. Reson.* 2:21–36.

42. Ulrich, A. S., A. Watts, I. Wallat, and M. P. Heyn. 1994. Distorted structure of the retinal chromophore in bacteriorhodopsin resolved by ^{2}H-NMR. *Biochemistry.* 33:5370–5375.

43. Ulrich, A. S., I. Wallat, M. P. Heyn, and A. Watts. 1995. Re-alignment of the retinal chromophore in the M-photointermediate of bacteriorhodopsin. *Nat. Struct. Biol.* 2:190–192.

44. Matsuzaki, K., Y. Mitani, K. Y. Akada, O. Murase, S. Yoneyama, M. Zasloff, and K. Miyajima. 1998. Mechanism of synergism between antimicrobial peptides magainin 2 and PGLa. *Biochemistry.* 37:15144–15153.

45. Wieprecht, T., O. Apostolov, M. Beyermann, and J. Seelig. 2000. Membrane binding and pore formation of the antibacterial peptide PGLa: Thermodynamic and mechanistic aspects. *Biochemistry.* 39:442–452.

46. Özdirekcan, S., D. T. S. Rijkers, R. M. J. Liskamp, and J. A. Killian. 2005. Influence of flanking residues on tilt and rotation angles of transmembrane peptides in lipid bilayers. A solid-state ^{2}H NMR study. *Biochemistry.* 44:1004–1012.

47. Zhou, N. E., B. Y. Zhu, B. D. Sykes, and R. S. Hodges. 1992. Relationship between amide proton chemical shifts and hydrogen bonding in amphipathic α-helical peptides. *J. Am. Chem. Soc.* 114:4320–4326.

48. Kuntz, I. D., P. A. Kosen, and E. C. Craig. 1991. Amide chemical shifts in many helices in peptides and proteins are periodic. *J. Am. Chem. Soc.* 113:1406–1408.

49. Toke, O., W. L. Maloy, S. J. Kim, J. Blazyk, and J. Schaefer. 2004. Secondary structure and lipid contact of a peptide antibiotic in phospholipid bilayers by REDOR. *Biophys. J.* 87:662–674.

50. Grage, S. L., and A. S. Ulrich. 2000. Orientation-dependent ^{19}F dipolar couplings within a trifluoromethyl-group are revealed by multipulse solid state NMR. *J. Magn. Reson.* 146:81–88.

51. Grage, S. L., J. Wang, T. A. Cross, and A. S. Ulrich. 2002. Structure analysis of fluorine-labeled tryptophan side chains in gramicidin A by solid state ^{19}F-NMR. *Biophys. J.* 83:3336–3350.